Published in final edited form as:
Integr Biol (Camb). 2011 September ; 3(9): 910–921. doi:10.1039/c1ib00043h.

In situ force mapping of mammary gland transformation

Jose I. Lopez[a], **Inkyung Kang**[†,a], **Weon-Kyoo You**[b], **Donald M. McDonald**[b], and **Valerie M. Weaver**[*,a,c]

[a]Department of Surgery and Center for Bioengineering and Tissue Regeneration, University of California at San Francisco, Department of Surgery, 513 Parnassus Ave, HSE 565, San Francisco, CA 94143-0456.

[b]Department of Anatomy, University of California at San Francisco, San Francisco, CA 94143

[c]Departments of Anatomy and Bioengineering and Therapeutic Sciences, Eli and Edythe Broad Center of Regeneration Medicine and Stem Cell Research and Helen Diller Family Comprehensive Cancer Center, University of California, San Francisco, San Francisco, CA 94143

Abstract

Tumor progression is characterized by an incremental stiffening of the tissue. The importance of tissue rigidity to cancer is appreciated, yet the contribution of specific tissue elements to tumor stiffening and their physiological significance remains unclear. We performed high-resolution atomic force microscopy indentation in live and snap-frozen fluorescently labeled mammary tissues to explore the origin of the tissue stiffening associated with mammary tumor development in PyMT mice. The tumor epithelium, the tumor-associated vasculature and the extracellular matrix all contributed to mammary gland stiffening as it transitioned from normal to invasive carcinoma. Consistent with the concept that extracellular matrix stiffness modifies cell tension, we found that isolated transformed mammary epithelial cells were intrinsically stiffer than their normal counterparts but that the malignant epithelium *in situ* was far stiffer than isolated breast tumor cells. Moreover, using an *in situ* vitrification approach, we determined that the extracellular matrix adjacent to the epithelium progressively stiffened as tissue evolved from normal through benign to an invasive state. Importantly, we also noted that there was significant mechanical heterogeneity within the transformed tissue both in the epithelium and the tumor-associated neovasculature. The vascular bed within the tumor core was substantially stiffer than the large patent vessels at the invasive front that are surrounded by the stiffest extracellular matrix. These findings clarify the contribution of individual mammary gland tissue elements to the altered biomechanical landscape of cancerous tissues and emphasize the importance of studying cancer cell evolution under conditions that preserve native interactions.

Introduction

Cancer is initiated by the acquisition of epigenetic, genetic and biochemical changes within the epithelium that enhance cell growth and survival and destabilize tissue integrity.[1–3] Tumor progression to malignancy is contingent on the transformed epithelium acquiring characteristics that enable cell migration and invasion into the tissue interstitial matrix.[4,5] In order to progress to malignancy, transformed epithelial cells must limit their interactions with neighboring cells and remodel and penetrate the extracellular matrix (ECM). The tumor

[*]Valerie.Weaver@ucsfmedctr.org; Fax: (415) 476-3985; Tel: (415) 476-3826.
[†]Current Address: Benaroya Research Institute at Virginia Mason, Seattle, WA 98101.

cells acquire a migratory and invasive phenotype allowing access to sites of dissemination such as the lymphatics and vasculature. Despite concerted effort, however, there is a scarcity of definitive molecular markers that predict which noninvasive tumors will progress to malignancy and which cancers will metastasize.

Comparative genomic hybridization and gene expression arrays, in which the genetic and transcriptional behavior of premalignant and invasive tumors have been compared, show surprisingly few differences, suggesting additional factors emanating from the tumor microenvironment must contribute to the pathogenesis of malignant progression.[6,7] Tissue angiogenesis, lymphangiogenesis, hypoxia and inflammation all appear to promote tumor aggression and metastasis.[8,9] Mechanical force and mechanical properties of the tissue also influence tumor progression and can promote the malignant behavior of tumors.[2] For instance, solid tumors have higher interstitial pressure than do normal tissues and this drives metastasis and enhances mortality by inducing hypoxia and compromising treatment efficacy.[10,11] Transformed tissues stiffen incrementally and experiments with transgenic animals suggest that this altered mechanical behavior contributes significantly to tumor progression and metastasis.[1,12] Thus, the mammary gland of the MMTV-PyMT/Col1a1 mouse has high tensile strength due to reduced collagen degradation and exhibits elevated metastasis.[13] Moreover, MMTV-ErbB2 mouse mammary gland tumors develop marked fibrosis and stiffening linked to collagen cross-linking mediated by lysyl oxidase (LOX) and inhibiting LOX activity in these animals reduced collagen cross-linking and tissue fibrosis and stiffening and decreased tumor incidence, functionally implicating tissue rigidity in tumor progression.[2] Neither of these studies however, distinguished between the effects of increased tissue level mechanical properties (bulk tissue stiffness and tensile strength) and local changes in ECM remodeling, increased tensile strength and stiffening on tumor progression and metastasis.[2]

Two (2D) and three-dimensional (3D) models attest to the importance of ECM stiffness as a regulator of growth, survival, migration and differentiation as well as stem cell fate and morphogenesis.[1,2,14–18] Reductionist *in vitro* approaches indicate that ECM stiffness mediates its cellular effects by modulating the activity of ion channels and transmembrane adhesion and growth factor receptors and by inducing cytoskeletal remodeling and actomyosin-dependent cell contractility.[1,12,15–18] Using a simple 3D organotypic culture model, we showed that ECM stiffness promotes the invasive behavior of an oncogenically pre-transformed mammary epithelium because it enhances integrin focal adhesion assembly and potentiates growth factor receptor signaling.[1,2,12,16] Attempts to establish whether similar molecular mechanisms promote tumor invasion *in vivo* have been hampered by the difficulty of spatially mapping localized tissue and ECM stiffening and assigning these changes to specific cellular morphologies and behaviors. Indeed, the mechanical properties of a tumor are complex and include elevated interstitial pressure and lymphatic flow, enhanced vascular and ECM remodeling and changes in cell mechanical properties and contractility relative to normal tissues.[2,12,19–21] Consequently, it remains unclear which of these biophysical parameters predominate in a tissue and at what time during tumor evolution they act and how.

Imaging modalities such as sonoelastography, MRI elastography and the tissue diagnostic instrument (TDI) have provided critical correlative data demonstrating that cancer tissue progressively stiffens.[22–28] These techniques possess unique diagnostic potential and have consistently served as a means to detect tumors and to illustrate a relationship between tissue stiffness and tumorigenesis. Nevertheless, their poor resolution and inability to distinguish between cellular and non-cellular tissue components limits their mechanistic utility. *In situ* methods to coordinately assess the biochemical and biomechanical evolution of living tumors are needed to obtain a comprehensive understanding of when and how mechanical

force influences the malignant transition of cancers and promotes tumor metastasis. Indeed, given the expanding range of cellular processes that biomechanical cues regulate, there is a pressing need to clarify the relevance of these cues to tumor behavior *in vivo* and to define plausible molecular mechanisms.

Atomic force microscopy (AFM) is a technique that has been used to image and characterize mechanical properties of living materials such as isolated cells at high resolution. Paradoxically, in contradiction to the growing body of evidence that tumors are stiffer than normal tissue, AFM analysis of immortalized cell lines as well as isolated primary tumor cells and pleural effusion biopsies suggest that metastatic lung, mammary and pancreatic cancer cells are softer than their normal counterparts.[29,30] Yet, no studies to date have characterized the mechanical properties of tumor cells in situations that preserve the context of the tumor epithelium within its native tissue. Obtaining this information is particularly important since cells tune their stiffness to reflect their local cellular and ECM microenvironment, and ECM stiffness and cell contractility have both been implicated in cell migration and metastasis.[18,31–34]

To address this issue, we used a well-characterized mouse model of mammary gland tumor progression that exhibits profound tumor metastasis in conjunction with transgenic CFP fluorescent labeling of the mammary epithelium. We combined this model with a method to fluorescently label the vasculature and an AFM *in situ* approach to explore the nature of biomechanical cues emanating from a mammary gland tissue as it evolved from normal to frank malignancy. Using these approaches we showed that the mammary gland epithelium, the tumor-associated vasculature and the adjacent ECM stiffen during mammary gland transformation. Moreover, ECM stiffening, which spatially registers with orientated collagen fibers, was a good gauge of biomechanical changes in transformed tissues that correlated with malignant progression.

Results

In situ biomechanical characterization of mammary gland tumors

Using unconfined compression analysis and shear rheometry, two methods routinely used to measure the bulk materials properties of tissue, we previously showed that the murine mammary gland progressively stiffens as it undergoes malignant transformation.[2] Although provocative, due to the low resolution of the bulk measurements used to analyze the biomaterials properties of the tissues in these studies, data derived from those experiments could not identify which tissue component contributed to tumor progression and stiffening. Not only do observations made from experiments conducted using these bulk tissue mechanical measurements obfuscate the source of the tissue stiffening but they also fail to assess the contribution of mechanical heterogeneity to tumor phenotype and progression.[35,36] Thus, it still remains unclear whether or not the stiffening associated with breast malignancy is linked to regional or global changes in the cellular component, changes in vascular density or local ECM remodeling and cross-linking.

AFM provides the spatial resolution necessary to distinguish between cellular and non-cellular tissue materials properties and is therefore ideally suited to tackle the issue of anatomical mechano-heterogeneity. Accordingly, we applied AFM to probe the biomechanical properties of mammary gland tissue *in situ* as it transformed from normal through to a fully invasive phenotype.

We chose the MMTV-PyMT mouse for our studies because it is a well-characterized model of mammary gland cancer that develops fully penetrant, multifocal mammary adenocarcinomas with short latency and high incidence of metastasis to the lymph nodes and

lung. The MMTV-PyMT mouse model closely resembles aggressive, estrogen and progesterone-negative ductal human breast cancer as demonstrated by the concomitant loss of estrogen and progesterone steroid hormone receptors and over expression of ErbB2 and cyclin D1 in late stage, invasive, metastatic tumors.[37–39]

We first applied phase contrast microscopy to identify mammary ducts and non-invasive/minimally invasive tumors from 10 week old mice and then performed AFM indentation force mapping on specified areas (Fig. 1A, red squares) within freshly excised mammary gland tissues (Fig. 1A, dashed lines). AFM analysis revealed that the elastic modulus of nontransformed, phenotypically normal mammary gland ducts was quite low with an average value of 0.4 kPa, whereas mammary tumors from the ten week old mice were significantly stiffer, averaging 1.2 kPa (Fig. 1A and B) ($P < 0.0001$). Interestingly, although all the tumors were consistently stiffer than normal tissue, we noted that the elastic modulus within individual tumors demonstrated considerable regional biomechanical heterogeneity. Although we consistently obtained values well under 0.4 kPa for normal mammary ducts, the stiffness measured within the transformed tissue varied by as much as 2.5 fold as the tissue progressed from a benign and minimally invasive state (ten week old mice) that had an average elastic modulus of 1.2 kPa, towards that of a frankly malignant and highly invasive tumor (14 week old mice) in which we measured an average elastic modulus of 3 kPa (Fig. 1B). The functional relevance of these biomechanical differences was demonstrated by our earlier studies which showed that inhibiting the activity of a collagen cross-linking enzyme lysyl oxidase (LOX) with β-aminopropionitrile (BAPN) reduced the bulk stiffness of the tissue and simultaneously delayed tumor progression and reduced tumor incidence.[2] In fact, analogous to the decrease in bulk tissue stiffness we measured previously in the Her2/Neu BAPN-treated animals, AFM quantification of the mechanical properties of BAPN-treated PyMT tumors from 14 week old mice revealed that the elastic modulus of the gland was significantly decreased and that the reduction in tissue stiffness was accompanied by a concomitant reduction in tumor metastasis (Fig. 1B; unpublished observations).

Mechanical properties of epithelial cells and vasculature differ in normal and malignant tissues

To address the contributions of individual anatomical components of the mammary tumor tissue to malignant behavior in the gland we used *in situ* labeling techniques to identify the epithelial cells, the vasculature and the extracellular matrix (ECM) and then assessed mechanical properties of each component. We employed PyMT mice with a fluorescently labeled epithelium, marked the vasculature using fluorescently-conjugated proteins, and identified the ECM using stains visualized by polarized light imaging.

We first assessed the biomechanical contribution of the tumor epithelium. We crossed the MMTV-PyMT mice with ACTB-ECFP fluorescent mice to generate animals in which the mammary epithelial cell lineage could be readily identified in non-fixed tissue using epifluorescence illumination and then quantified the stiffness of the epithelium using AFM. *In situ* AFM analysis confirmed that the normal mammary ductal epithelium was quite soft (~0.25 kPa) and that on average the tumor epithelium of the 10 week old mouse was at least 3-fold stiffer (~0.8 kPa; Fig. 2A and B).[2,12] However, in light of previously published data indicating that metastatic, mammary tumor cells isolated from pleural effusion are significantly softer than their non-transformed counterparts, we also isolated fresh populations of primary normal mammary epithelial cells and compared their materials properties to primary tumor epithelial cells isolated from PyMT tumors *ex vivo*.[29,30] Our objective was to determine whether primary breast tumor cells are intrinsically stiffer than their normal counterparts, and furthermore, to ascertain whether the tumor microenvironment contributes to the biomechanical phenotype of the epithelium.

We noted that the Young's elastic modulus of freshly isolated transformed mammary epithelial cells was significantly higher (0.3 kPa) than that of age matched normal counterparts (0.2 kPa). Yet, AFM indentation showed that the isolated tumor epithelial cells were significantly softer (0.3 kPa) than the tumor epithelium measured *in situ* (0.8–1.2 kPa; left bars compared to right bars, Fig. 2B). Thus, malignant transformation increased the stiffness of mammary epithelial cells but our measurements demonstrated that the tissue microenvironment and cellular context contributed substantially to the mechanical phenotype of the transformed epithelium.

We next assayed the biomechanical contribution of the tumor-associated vasculature by perfusing 10 week old ACTB-ECFP/MMTV-PyMT animals with rhodamine-labeled lectin (Rh-lectin) to label patent blood vessels. We then sacrificed the animals and quantified the materials properties of the vessels in the freshly dissected tissues using AFM (Fig. 3A). Using this approach, the Rh-lectin tagged vascular component of the tissue was readily visualized and we were able to accurately spatially map and quantify their material properties using AFM (Fig. 3A, dashed lines). We also verified the tissue origin and phenotype of the vessels within these mechanically analyzed tissues by immunostaining for vascular markers and quantifying vessel diameter and organization (Fig. 3A, right bar graph). Consistent with the notion that the vascular component of the stroma contributes to the increased stiffness measured in these tumors, AFM indentation measurements indicated that the Rh-lectin labeled patent blood vessels were much stiffer than vessels adjacent to the mammary ducts within normal tissue. Interestingly, we also noted that there was considerable mechanical heterogeneity within the vascular beds in these developing mammary tumors. Thus, although AFM analysis confirmed that tumor-associated blood vessels were significantly stiffer than blood vessels found in normal mammary tissue (Fig. 3B), the vascular component associated with the center of the PyMT tumors was much stiffer than the blood vessels located at the invasive front of the lesions (Fig. 3; $P < 0.05$). This biomechanical heterogeneity was accompanied by morphological and functional differences in the vasculature such that the vessels at the invasive front were largely patent (revealed by CD31 and Rh-lectin positive staining) and had larger average vessel diameters ($18 \pm 4.5\ \mu m$). By contrast, the average diameter of the vessels within the tumor core was considerably smaller ($12 \pm 4.2\ \mu m$) and in many instances the vessels were CD31 positive but Rh-lectin negative, suggesting they were no longer functional.[40,41] These data are consistent with prior studies demonstrating that the architectural features of the vasculature within the core of tumors differs from those located at the invasive front.[42,43] The findings also illustrated that this morphological and functional heterogeneity was reflected by quantifiable differences in the mechanical properties of these vessels as revealed by AFM (Fig. 3B).

Mammary gland vitrification permits spatial assessment of the mechanical properties of the tissue extracellular matrix

To examine the contribution of ECM remodeling to tumor stiffening and the biomechanical heterogeneity of the ECM in mammary gland lesions, we developed a vitrification preparation protocol that permitted the accurate mechanical profiling of the ECM in cryosections of tissue. This approach entailed the rapid freezing/thawing of mammary gland tissue while preserving the architecture and biomechanical properties of live mammary gland specimens.

We first tested the effect of rapid *versus* slow freezing on mammary extracellular matrix integrity and stiffness. We excised fresh mammary glands and either quickly froze them *in situ* by rapidly immersing the tissue in liquid nitrogen or froze them slowly within custom-made chambers by progressively cooling samples in isopropanol chilled to −20 °C followed by chilling in −80 °C isopropanol prior to final immersion in liquid nitrogen. We then

examined the effect of either slowly thawing the tissue at room temperature or rapidly thawing the tissue by immersing the frozen specimen within large quantities of room temperature phosphate buffered saline (PBS) supplemented with protease inhibitors. We measured a dramatic decrease in the Young's elastic modulus in those mammary gland tissues that had been slowly frozen and/or slowly thawed (average 60% decrease; Fig. 4A, graph). We also noted that these same tissues exhibited striking architectural disturbances as compared to their never frozen counterparts that were consistent with the freeze damage associated with water crystallization and expansion (Fig. 4A). Microscopy examination of mammary gland tissue subjected to slow freeze/thawing also revealed that adipose tissue was ruptured, tissue volume was decreased, optical clarity of the tissue was enhanced and the tissue margins were compromised. By contrast, the elastic modulus of the tissue that was rapidly frozen and thawed was remarkably preserved and had not significantly changed from its non-frozen native state (Fig. 4A, graph). The architectural integrity of the rapidly frozen and thawed tissue was essentially maintained: The morphology of the adipocyte component and epithelium remained essentially unchanged, the optical density of the tissue pre- and post-freezing was comparable, and the tissue borders remained markedly defined (Fig. 4A). AFM indentation measurements conducted pre- and post-freezing also revealed that regardless of the initial stiffness of the tissue there was a mere 6 percent change in the Young's elastic modulus in tissues that were rapidly frozen and thawed, whereas slow-freeze/slow-thawed tissue or rapid-freeze/slow thawed tissue showed 38 and 52 percent reductions in the Young's elastic moduli, respectively (Fig. 4B).

To verify the AFM indentation measurement results, we rapidly froze and thawed the mammary gland tissue and conducted repeat elasticity measurements at precisely the same geographic location within the tissue by vitrifying and thawing the tissue on the AFM stage. Despite minor differences in the optical clarity of the tissue, we noted that the integrity of these cryo-manipulated tissues remained intact, as indicated by retention of adipocyte architecture as well as maintenance of gross tissue shape and morphology (Fig. 4C). We also observed that the elastic modulus measurements obtained before and after repeat freeze/thaw cycles remained essentially unchanged; average variation was a mere 7 percent (Fig. 4C). This novel tissue vitrification approach thus preserved the mechanical and morphological integrity of mammary tissue.

In situ force mapping of mammary gland ECM during transformation

We applied our vitrification approach to spatially map the materials properties of the ECM in the PyMT mice as they transitioned from normal through to frankly invasive lesions. We rapidly froze and rapidly thawed tissue sections excised from normal, premalignant and malignant tissues obtained from MMTV-PyMT mouse mammary glands and conducted in-depth AFM indentation mapping of the ECM associated with the terminal ductal lobular units and evolving mammary tumor lesions. To differentiate cellular material from the ECM we stained cell nuclei with the permeable dye Hoechst 3332 and visualized the ECM after AFM mapping using phase-contrast microscopy imaging followed by picrosirius red staining and polarized light imaging. Positioning of the AFM indentor at multiple locations within the interface between the tumor epithelium and the stroma (Fig. 5A, red boxes) permitted the generation of multiple 90 × 90 μm spatially-targeted force maps within the ECM of mammary tissue. This strategy also permitted us to quantify the mechanical heterogeneity of the ECM within the transforming gland.

As the mammary epithelium progressed from normal, to premalignant and to invasive malignant tumors, there was a progressive increase in the Young's elastic modulus, particularly within the ECM adjacent to and surrounding each invasive tumor epithelium (Fig. 5A, force maps). The Young's elastic modulus of the ECM surrounding the ductal

epithelium increased from an average of 1.1 kPa in the normal duct, to 1.3 kPa in pre-malignant tumors and to 1.7 kPa in the malignant tumors (Fig. 5C).

Collagen is the most abundant protein present within ECM and contributes significantly to biomechanical tissue integrity.[44] Post-hoc histological quantification of orthogonally polarized light micrographs of picrosirius red staining of the tissue revealed that there was a significant increase in fibrillar collagen deposition as the gland transformed (Fig. 5A; quantified in Fig. 5B). However, although the fibrillar collagen stiffened as the gland evolved from a premalignant to a frankly invasive state, we did not quantify a further increase in collagen deposition. These findings suggest that additional factors such as collagen cross-linking, linearization and deposition and increased expression of other ECM proteins must contribute to further ECM stiffening as the tissue transitions to frank malignancy.[45,45]

Discussion

Here we employed an *in situ* AFM-based approach to quantify and spatially characterize the biomechanical properties of freshly excised, intact mammary gland tissue as it transformed from normal to frank malignancy. The influence of biomechanics on tumor epithelial cell behavior is recognized; however analysis of the relationship between cell and tissue stiffening to cancer progression at the molecular scale and in living tissues has been technically challenging. Sonoelastography, MRI elastography, TDI analysis and physical palpation leave no doubt that the pathogenesis of invasive mammary cancer is associated with tissue stiffening.[22–28] Multiple factors clearly contribute to tissue stiffening in tumors including elevated interstitial pressure and compression, enhanced cell contractility and elevated tumor cell mass as well as increased vascular density and ECM deposition, cross-linking and remodeling.[2,12,19–21] Yet, the limited resolution of imaging modalities has compromised the use of these approaches to clarify the molecular basis for the biomechanical changes in cancerous tissue.

Using a combination of genetic and molecular fluorescent tagging with AFM and a novel tissue vitrification approach, we physically quantified and characterized the nature of the biomechanical stiffening associated with tumor progression in an experimental model of mammary gland cancer. We also found there was a coordinate stiffening of the ECM and the epithelium as the mammary gland transitioned from normal tissue to frank malignancy. Tumorigenesis is associated with an increase in microvascular density;[42,43] and we determined that the vasculature associated with the developing tumors was stiffer than the vasculature of normal tissue. Our data also demonstrated that there were inherent differences in the mechanical properties of the vasculature within the tumor core *versus* the vessels at the invasive front. Indeed, we found that these different mechanical phenotypes in the vascular beds were associated with quantifiable changes in the morphology and functional behavior of the vessels. By exploiting high-resolution AFM we also uncovered inherent biomechanical heterogeneities within the epithelium and the ECM of cancerous tissue. Thus, not only do our data clarify the anatomical components contributing to tumor stiffening but our findings also raise the possibility that mechanical heterogeneity within tumors could contribute to the heterogeneous behavior of some cancers.[46–48] Therefore our approach offers a high-resolution strategy with which to clarify and study the role of biomechanical heterogeneity in cancer progression.

Our *in situ* AFM force mapping studies using double transgenic MMTV-PyMT/ACTB-ECFP mice showed that mammary epithelial cell stiffness increased at least three-fold as the epithelium transformed from normal to frankly invasive lesions (Fig. 2B). The findings demonstrate that the tumor epithelium is a significant biomechanical contributor to the

overall stiffening of the transformed tissue. The results agree with prior bulk property analyses of transformed mouse and human tumor tissue and are consistent with the idea that cells "tune" their mechanical properties in response to their mechanical microenvironment.[49,50] In marked contradiction to our findings however, prior work suggested that the mechanical properties of isolated cancer cells are, paradoxically, softer than non-transformed cells and imply that this 'softer phenotype' is a prerequisite for tumor metastasis.[29,30] Such findings are at odds with *in vivo* imaging studies that clearly demonstrate that solid tumors are significantly stiffer than normal tissue, and that tissues incrementally stiffen with cancer progression.[22–28] Indeed, intravital microscopy imaging of metastasizing mammary gland tumor epithelium illustrate how tumor cells disseminate from primary tumors and migrate along thick and presumably "stiff" collagen fibers; through a process that culture manipulations suggest is favored by high traction forces and elevated tumor cell mechano-responsiveness (Lopez *et al.*, unpublished observations).[18,32,34] One major difference between these prior *in vitro* cellular rheology findings and our current study is that our measurements were conducted *in situ* under conditions in which heterotypic and homotypic cellular interactions and ECM associations were strictly maintained. These conditions impart critical biochemical and biomechanical constraints on cellular behavior. For instance, epithelial cells sense and respond to the mechanical compliance of the microenvironment by pulling on their surroundings in an actomyosin-dependent fashion that alters the cells intrinsic stiffness.[49,50] Our AFM indentation experiments demonstrated that although isolated mammary epithelial tumor cells were stiffer than normal mammary epithelial cells they were substantially softer when measured *ex vivo* than *in situ* (Fig. 2B). Previous work in which the rheology of metastatic tumor cells was characterized examined isolated pleural effusion or tumor cells which by definition lack biochemical and physical connections to surrounding tissue elements.[29,30] By contrast, the current study examined the mechanical properties of tumor cells *in situ*, under conditions that preserve the native cellular associations between the tumor cells and the surrounding microenvironment.

Importantly, while there was a consistent overall increase in tumor cell stiffness, we also noted that there was considerable biomechanical heterogeneity within the epithelium of each tumor (Fig. 2B). The heterogeneous mechanical properties of the cancer cells within each tumor mass could reflect the non-uniform state of the local cellular and extracellular microenvironment including whether or not the tumor cells were adjacent to a necrotic region or were proximal to a blood vessel or collagen fibril.[49,50] Alternatively, this heterogeneity could be due to cell intrinsic properties linked to either an inherent genetic heterogeneity that enhances cellular contractility or differential mechanical properties of cells from distinct origins. It is tempting to speculate that the observed biomechanical tumor cell heterogeneity could reflect the unique mechanical behavior of a subpopulation of tumor stem or progenitor cells, especially given recent evidence that stem cells are softer and exhibit differential biomechanical behaviors than their differentiated progeny.[51–53]

Tumor progression is intimately linked to angiogenesis and we observed changes in vascular mechanical properties as mammary tumors developed.[42,43] AFM force mapping revealed the two distinct types of tumor-associated vasculature. We noted that the vasculature associated with the tumor core was quite stiff, stiffer even than the surrounding transformed epithelium and that the vasculature at the tumor front was by contrast relatively soft (Fig. 3A and B). The rigidity of the vasculature at the tumor core might reflect either differences in the maturity of the vasculature or physical changes in the intra-tumoral vessels that have collapsed due to high solid stresses exerted by the proliferating tumor mass or interstitial tumor pressure.[11,42,54] CD31 immunofluorescent staining of Rh-lectin perfused mammary tumors revealed non-patent vessels within the tumor core and leaky vessels at the invasive front of the tumors (Fig. 3C) that are typical of the different types of vessels found in aggressive tumors.[42,43] It is feasible that differences in the biomechanical properties of these

vessels reflect the maturity and perfusion of these vessels. Regardless, immature vessels and collapsed vessels compromise the transport of cytotoxic cancer therapeutic drugs, and increased tumor stiffness is a primary impediment to efficient drug delivery.[54]

Interestingly, the soft neovasculature at the invasive front of tumors was located within a region of the ECM that was quite stiff. Previous work has demonstrated that a very stiff ECM compromises vascular integrity possibly by inhibiting vascular endothelial pseudopodial branch initiation and disrupting vascular network assembly, implicating ECM rigidity as a key regulator of vasculature heterogeneity.[55–57] Whether ECM stiffness could actively promote disease progression and induce drug resistance by regulating the phenotype of the tumor-associated vasculature awaits further “mechanistic” analysis.

To establish the relationship between ECM biomechanical property changes and tumor progression necessitated the development of new *in situ* approaches in which the ECM could be accurately identified and the biochemical and morphological makeup of the spatially-probed region comprehensively analyzed. Consequently, a rapid freeze/rapid thaw tissue vitrification approach was developed to preserve the biomechanical integrity of the tissue so that tissues were amenable for sectioning, and thus precise positioning of the AFM probe to the ECM could be achieved (Fig. 4). Although freezing and vitrification have been previously used to preserve the integrity of both stiff and soft tissues such as bone and cartilage, as well as skin and adipose, it had not been coupled to AFM force mapping.[58–62] Similarly, AFM has been used previously to visualize the characteristics of heart, cornea, liver and bone tissues at a micro and nano-scale and in rare instances to obtain low-resolution mechanical information.[63–67] However, until our study AFM was never coupled with traditional histopathologic methods to register the molecular and cellular composition and behavior of the tissue that was being force mapped. Through the application of tissue vitrification we were able to examine the morphological and mechanical behavior of the ECM in the mammary gland as it transitioned from the normal to the cancerous state. Using this approach we confirmed that the ECM progressively stiffened during tumor progression (Fig. 5C). Although collagen-dense breast tissue has been associated with increased risk to breast malignancy, a casual link between altered collagen deposition and tissue mechanical properties in breast cancer progression has not been explored.[22–28,68–70] This is primarily due to the fact that until our study no *in situ* approach existed to accurately mechanically and histopathogically examine tissues at high resolution. Using AFM histopathologic examination we were able to demonstrate that while the fibrillar collagen stiffened during tumor progression, collagen deposition alone was not able to account for the observed biomechanical stiffening. Instead our findings suggest that ECM remodeling, altered crosslinking, fibril linearization and orientation also must contribute to increased ECM mechanical properties.[12]

Our findings are consistent with and extend prior work from our group and others strongly implicating collagen remodeling and stiffening in mammary gland tumor transition to invasion and metastasis.[2,12,13,71] Indeed, the fact that we noted consistent stiffening during tumor progression suggests that the oriented, thickened collagen fibers along which mammary gland tumor cells have been seen to migrate are indeed a source of the ECM stiffening and suggest that these biomaterials properties facilitate tumor cell invasion and metastasis.[13,72,73] Interestingly, protein degradation mediated by matrix metalloproteinases (MMPs) has been implicated in tumor progression and metastasis and an overwhelming body of evidence support the contention that MMPs are absolutely critical for fostering the transition of oncogenically-transformed epithelia to an invasive phenotype.[74,75] Our observation that invasive mammary gland tumors are characterized by a stiffened ECM suggests that perhaps MMPs play a more nuanced role in fomenting tumor progression by

"remodeling" and creating rigid collagen fibrils that foster tumor cell migration and invasion into the interstitial matrix; this possibility must be rigorously tested.

This study provides important new insight into the interplay between tumor evolution and the biomechanics of cancer. Nevertheless many questions remain, not the least of which is whether or not different subtypes of mammary gland tumors (basal, luminal, ER/PR positive, Her2 positive) evolve within unique biomechanical microenvironments that foster their histophenotype and behavior. Moreover, it is not obvious whether there exist temporal- and cell-type specific biomechanical hierarchies within a tissue and if so whether and how these physical parameters influence tumor evolution. What is clear is that at present we lack the ability to predict which tumors will progress to malignancy and which will be most lethal.[76,77] Perhaps by clarifying the role of biomechanics in tumorigenesis at the micro-scale we will obtain the critical information required to clarify this dilemma. Our findings suggest that tumor and ECM stiffness may be novel prognostic metrics that could indicate whether or not a noninvasive lesion will progress. The next challenge will be to develop tractable approaches to accurately image and quantify these physical changes so that they can be translated to the clinic.

Experimental

Mice and tissues

FVB-TgN MMTV-PyMT[37] (Jackson Laboratory) and FVB-TgN ACTB-ECFP[78] (kindly provided by Z. Werb) mice were maintained in accordance with the University of California Institutional Animal Care and Use Committee guidelines. The presence of mammary gland lesions were detected by physical palpation (at ~3 mm) and malignancy state was confirmed by histological analysis following H&E staining. Animals were sacrificed between 7–14 weeks of age at which time mammary glands and tumors were excised and subdivided. In some experiments, animals were anesthetized (ketamine) and intravenously injected with rhodamine-labeled *Lycospericon esculentum* lectin (100 μg in 100 μl 0.9% NaCl; Vector Labs) followed by perfusion (30 min) with PBS prior to sacrifice.[79] Mammary glands were either analyzed immediately after harvesting or following cryopreservation. Frozen glands were embedded in OCT (Tissue-Tek) aqueous embedding compound within a disposable plastic base mold (Fisher) and immersed into isopropanol chilled to −20 °C, then isopropanol chilled to −80 °C, and then in liquid N_2 or were snap frozen by direct immersion into liquid nitrogen. Frozen tissue blocks were then cut into 20-μm sections using disposable low profile microtome blades (Leica, 819) on a cryostat (Leica, CM1900-3-1). Eighteen animals were used for AFM quantification of tumor epithelium and Young's elastic modulus and 12 animals were perfused for AFM quantification of vascular Young's elastic modulus.

AFM

All AFM indentations were performed using an MFP3D-BIO inverted optical AFM mounted on a Nikon TE2000-U inverted fluorescent microscope (Asylum Research). Pyramidal silicon nitride cantilevers with a spring constant of 0.06 N m^{-1} were custom fitted with borosilicate glass spheres 5 μm in diameter (Novascan Tech) and calibrated using the thermal noise method prior to each experiment.[80] Samples were indented with a calibrated force of 5 nN and the Hertz model[81] of impact was used to determine the elastic properties of the tissue (E_1). AFM force maps were typically obtained as a 10 × 10 raster series of indentations utilizing the FMAP function of the IGOR PRO build supplied by Asylum Research. Cells were assumed to be incompressible and a Poisson's ratio of 0.5 was used in the calculation of the Young's elastic modulus.[82]

Histology

Freshly excised mammary glands and tumors were fixed post-AFM indentation in 10% neutral buffered formalin. Tissue sections were stained using 0.1% picrosirius red (Direct Red 80, Sigma) and counterstained with Weigert's hematoxylin. Sections were imaged using an Olympus IX81 fluorescent microscope fitted with an analyzer (U-ANT) and polarizer (U-POT, Olympus) oriented parallel and orthogonal to each other. Images were quantified with minimal thresholding in ImageJ.

Statistics

Statistical analysis was performed using GraphPad Prism V5.0c. Statistical significance was assessed using either a two-tailed unpaired Student's *t*-test or two-way ANOVA. Means are presented as ±SEM of multiple measurements and statistical significance was considered at $P < 0.05$.

Acknowledgments

We thank Ryan Giles for writing the Java code for AFM Hertz model fitting and analysis and Johnathon Lakins for helpful discussions and technical guidance. This work was supported by a DOD BCRP grant W81XWH-05-1-0330 and NCI grants U54CA143836-01 and CA138818-01A1 to VMW and NIH grant 1U01ES009458-01 to ZW as well as an IRACDA Scholars in Science K12GM081266 award to JIL.

References

1. Butcher DT, Alliston T, Weaver VM. A tense situation: forcing tumour progression. Nat. Rev. Cancer. 2009; 9:108–122. [PubMed: 19165226]
2. Levental KR, et al. Matrix crosslinking forces tumor progression by enhancing integrin signaling. Cell. 2009; 139:891–906. [PubMed: 19931152]
3. Polyak K. Breast cancer gene discovery. Expert Rev. Mol. Med. 2002; 4:1–18. [PubMed: 14987381]
4. Chambers AF, Groom AC, MacDonald IC. Dissemination and growth of cancer cells in metastatic sites. Nat. Rev. Cancer. 2002; 2:563–572. [PubMed: 12154349]
5. Wiseman BS, Werb Z. Stromal effects on mammary gland development and breast cancer. Science. 2002; 296:1046–1049. [PubMed: 12004111]
6. Climent J, Garcia JL, Mao JH, Arsuaga J, Losada J. Perez. Characterization of breast cancer by array comparative genomic hybridization. Biochem. Cell Biol. 2007; 85:497–508. [PubMed: 17713584]
7. Pedraza V, et al. Gene expression signatures in breast cancer distinguish phenotype characteristics, histologic subtypes and tumor invasiveness. Cancer. 2010; 116:486–496. [PubMed: 20029976]
8. Avraamides CJ, Susini B. Garmy, Varner JA. Integrins in angiogenesis and lymphangiogenesis. Nat. Rev. Cancer. 2008; 8:604–617. [PubMed: 18497750]
9. Nguyen DX, Bos PD, Massague J. Metastasis: from dissemination to organ-specific colonization. Nat. Rev. Cancer. 2009; 9:274–284. [PubMed: 19308067]
10. Stohrer M, Boucher Y, Stangassinger M, Jain RK. Oncotic pressure in solid tumors is elevated. Cancer Res. 2000; 60:4251–4255. [PubMed: 10945638]
11. Swartz MA, et al. Mechanics of interstitial-lymphatic fluid transport: theoretical foundation and experimental validation. J. Biomech. 1999; 32:1297–1307. [PubMed: 10569708]
12. Paszek MJ, Boettiger D, Weaver VM, Hammer DA. Integrin clustering is driven by mechanical resistance from the glycocalyx and the substrate. PLoS Comput. Biol. 2009; 5:e1000604. [PubMed: 20011123]
13. Provenzano P, et al. Collagen density promotes mammary tumor initiation and progression. BMC Med. 2008; 6:11. [PubMed: 18442412]
14. Paszek MJ, et al. Tensional homeostasis and the malignant phenotype. Cancer Cell. 2005; 8:241–254. [PubMed: 16169468]

15. Dyachenko V, Christ A, Gubanov R, Isenberg G. Bending of z-lines by mechanical stimuli: an input signal for integrin dependent modulation of ion channels? Prog. Biophys. Mol. Biol. 2008; 97:196–216. [PubMed: 18367237]
16. Yeung T, et al. Effects of substrate stiffness on cell morphology, cytoskeletal structure, and adhesion. Cell Motil. Cytoskeleton. 2005; 60:24–34. [PubMed: 15573414]
17. Tee S-Y, Bausch AR, Janmey PA. The mechanical cell. Curr. Biol. 2009; 19:R745–748. [PubMed: 19906576]
18. Discher DE, Janmey P, Wang Y-L. Tissue cells feel and respond to the stiffness of their substrate. Science. 2005; 310:1139–1143. [PubMed: 16293750]
19. Kumar S, Weaver VM. Mechanics malignancy and metastasis: the force journey of a tumor cell. Cancer Metastasis Rev. 2009; 28:113–127. [PubMed: 19153673]
20. Fukumura D, Duda DG, Munn LL, Jain RK. Tumor microvasculature and microenvironment: novel insights through intravital imaging in pre-clinical models. Microcirculation. 2010; 17:206–225. [PubMed: 20374484]
21. Fukumura D, Jain RK. Tumor microenvironment abnormalities: causes consequences, and strategies to normalize. J. Cell. Biochem. 2007; 101:937–949. [PubMed: 17171643]
22. Hansma P, et al. The tissue diagnostic instrument. Rev. Sci. Instrum. 2009; 80:054303. [PubMed: 19485522]
23. Qiu Y, Insana MF. Ultrasonic viscoelasticity imaging of nonpalpable breast lesions. Conf. Proc. IEEE Eng. Med. Biol. Soc. 2009:4424–4427. [PubMed: 19963829]
24. Sinkus R, et al. Viscoelastic shear properties of in vivo breast lesions measured by MR elastography. Magn. Reson. Imaging. 2005; 23:159–165. [PubMed: 15833607]
25. Thomas A, et al. Significant differentiation of focal breast lesions: calculation of strain ratio in breast sonoelastography. Acad. Radiol. 2010; 17:558–563. [PubMed: 20171905]
26. Samani A, Bishop J, Luginbuhl C, Plewes DB. Measuring the elastic modulus of ex vivo small tissue samples. Phys. Med. Biol. 2003; 48:2183–2198. [PubMed: 12894978]
27. Xydeas T, et al. Magnetic resonance elastography of the breast: correlation of signal intensity data with viscoelastic properties. Invest. Radiol. 2005; 40:412–420. [PubMed: 15973132]
28. Chung SY, et al. Differentiation of benign from malignant nonpalpable breast masses: a comparison of computer-assisted quantification and visual assessment of lesion stiffness with the use of sonographic elastography. Acta Radiol. 2010; 51:9–14. [PubMed: 19929254]
29. Li QS, Lee GYH, Ong CN, Lim CT. AFM indentation study of breast cancer cells. Biochem. Biophys. Res. Commun. 2008; 374:609–613. [PubMed: 18656442]
30. Cross SE, Jin Y-S, Rao J, Gimzewski JK. Nanomechanical analysis of cells from cancer patients. Nat. Nanotechnol. 2007; 2:780–783. [PubMed: 18654431]
31. Isenberg BC, DiMilla PA, Walker M, Kim S, Wong JY. Vascular smooth muscle cell durotaxis depends on substrate stiffness gradient strength. Biophys. J. 2009; 97:1313–1322. [PubMed: 19720019]
32. Wang W, et al. Single cell behavior in metastatic primary mammary tumors correlated with gene expression patterns revealed by molecular profiling. Cancer Res. 2002; 62:6278–6288. [PubMed: 12414658]
33. Samuel MS, et al. Tissue selective expression of conditionally-regulated ROCK by gene targeting to a defined locus. Genesis. 2009; 47:440–446. [PubMed: 19391117]
34. Winer JP, Oake S, Janmey PA. Non-linear elasticity of extracellular matrices enables contractile cells to communicate local position and orientation. PLoS One. 2009; 4:e6382. [PubMed: 19629190]
35. Baker EL, Lu J, Yu D, Bonnecaze RT, Zaman MH. Cancer cell stiffness: integrated roles of three-dimensional matrix stiffness and transforming potential. Biophys. J. 2010; 99:2048–2057. [PubMed: 20923638]
36. Ingber DE. Can cancer be reversed by engineering the tumor microenvironment? Semin. Cancer Biol. 2008; 18:356–364. [PubMed: 18472275]

37. Guy CT, Cardiff RD, Muller WJ. Induction of mammary tumors by expression of polyomavirus middle T oncogene: a transgenic mouse model for metastatic disease. Mol. Cell. Biol. 1992; 12:954–961. [PubMed: 1312220]
38. Lin EY, et al. Progression to malignancy in the polyoma middle T oncoprotein mouse breast cancer model provides a reliable model for human diseases. Am. J. Pathol. 2003; 163:2113–2126. [PubMed: 14578209]
39. Maglione JE, et al. Transgenic Polyoma middle-T mice model premalignant mammary disease. Cancer Res. 2001; 61:8298–8305. [PubMed: 11719463]
40. Huang F-J, et al. Pericyte deficiencies lead to aberrant tumor vascularizaton in the brain of the NG2 null mouse. Dev. Biol. 2010; 344:1035–1046. [PubMed: 20599895]
41. You W-K, Kasman I, Lowe D. D. Hu, McDonald DM. Ricinus communis agglutinin I leads to rapid down-regulation of VEGFR-2 and endothelial cell apoptosis in tumor blood vessels. Am. J. Pathol. 2010; 176:1927–1940. [PubMed: 20185574]
42. Carmeliet P, Jain RK. Angiogenesis in cancer and other diseases. Nature. 2000; 407:249–257. [PubMed: 11001068]
43. Gupta GP, et al. Mediators of vascular remodelling co-opted for sequential steps in lung metastasis. Nature. 2007; 446:765–770. [PubMed: 17429393]
44. á , L. Kolácn, et al. Biochemical and biophysical aspects of collagen nanostructure in the extracellular matrix. Physiol. Res. 2007; 56(Suppl 1):S51–60. [PubMed: 17552894]
45. Junqueira LC, Montes GS, Sanchez EM. The influence of tissue section thickness on the study of collagen by the Picrosirius-polarization method. Histochemistry. 1982; 74:153–156. [PubMed: 7085347]
46. Ingber DE. Cancer as a disease of epithelial–mesenchymal interactions and extracellular matrix regulation. Differentiation. 2002; 70:547–560. [PubMed: 12492496]
47. Levental I, Georges PC, Janmey PA. Soft biological materials and their impact on cell function. Soft Matter. 2007; 3:299.
48. Kuwada SK, Li X. Integrin alpha5/beta1 mediates fibronectin-dependent epithelial cell proliferation through epidermal growth factor receptor activation. Mol. Biol. Cell. 2000; 11:2485–2496. [PubMed: 10888683]
49. Pelham RJ, Wang Y.-li. Cell locomotion and focal adhesions are regulated by substrate flexibility. Proc. Natl. Acad. Sci. U. S. A. 1997; 94:13661–13665. [PubMed: 9391082]
50. Engler A, et al. Substrate compliance versus ligand density in cell on gel responses. Biophys. J. 2004; 86:617–628. [PubMed: 14695306]
51. Greenberg AW, Hammer DA. Cell separation mediated by differential rolling adhesion, Biotechnol. Bioeng. 2001; 73:111–124.
52. Huebsch N, et al. Harnessing traction-mediated manipulation of the cell/matrix interface to control stem-cell fate. Nat. Mater. 2010; 9:518–526. [PubMed: 20418863]
53. Engler AJ, Sen S, Sweeney HL, Discher DE. Matrix elasticity directs stem cell lineage specification. Cell. 2006; 126:677–689. [PubMed: 16923388]
54. Padera TP, et al. Pathology: Cancer cells compress intratumour vessels. Nature. 2004; 427:695. [PubMed: 14973470]
55. Califano JP, King C. A. Reinhart. The effects of substrate elasticity on endothelial cell network formation and traction force generation. Conf. Proc. IEEE Eng. Med. Biol. Soc. 2009:3343–3345. 2009. [PubMed: 19964074]
56. Fischer RS, Gardel M, Ma X, Adelstein RS, Waterman CM. Local cortical tension by Myosin II guides 3D endothelial cell branching. Curr. Biol. 2009; 19:260–265. [PubMed: 19185493]
57. Sieminski AL, Hebbel RP, Gooch KJ. The relative magnitudes of endothelial force generation and matrix stiffness modulate capillary morphogenesis in vitro. Exp. Cell Res. 2004; 297:574–584. [PubMed: 15212957]
58. Chan RW, Tize IR. Effect of postmortem changes and freezing on the viscoelastic properties of vocal fold tissues. Ann. Biomed. Eng. 2003; 31:482–491. [PubMed: 12723689]
59. Foutz TL, Stone EA, Abrams CF. Effects of freezing on mechanical properties of rat skin. Am. J. Vet. Res. 1992; 53:788–792. [PubMed: 1524309]

60. Geerligs M, Peters GWM, Ackermans PAJ, Oomens CWJ, Baaijens FPT. Linear viscoelastic behavior of subcutaneous adipose tissue. Biorheology. 2008; 45:677–688. [PubMed: 19065014]
61. Kang Q, An YH, Friedman RJ. Effects of multiple freezing-thawing cycles on ultimate indentation load and stiffness of bovine cancellous bone. Am. J. Vet. Res. 1997; 58:1171–1173. [PubMed: 9328673]
62. Kiefer GN, et al. The effect of cryopreservation on the bio-mechanical behavior of bovine articular cartilage. J. Orthop. Res. 1989; 7:494–501. [PubMed: 2738767]
63. Thurner PJ. Atomic force microscopy and indentation force measurement of bone. Wiley Interdiscip. Rev. Nanomed. Nanobiotechnol. 2009; 1:624–649. [PubMed: 20049821]
64. Gang Z, Qi Q, Jing C, Wang C. Measuring microenvironment mechanical stress of rat liver during diethylnitrosamine induced hepatocarcinogenesis by atomic force microscope. Microsc. Res. Tech. 2009; 72:672–678. [PubMed: 19353647]
65. Last JA, Liliensiek SJ, Nealey PF, Murphy CJ. Determining the mechanical properties of human corneal basement membranes with atomic force microscopy. J. Struct. Biol. 2009; 167:19–24. [PubMed: 19341800]
66. Engler AJ, Rehfeldt F, Sen S, Discher DE. Microtissue elasticity: measurements by atomic force microscopy and its influence on cell differentiation. Methods Cell Biol. 2007; 83:521–545. [PubMed: 17613323]
67. Engler AJ, et al. Embryonic cardiomyocytes beat best on a matrix with heart-like elasticity: scar-like rigidity inhibits beating. J. Cell Sci. 2008; 121:3794–3802. [PubMed: 18957515]
68. McCormack VA, Silva I. dos Santos. Breast density and parenchymal patterns as markers of breast cancer risk: a meta-analysis. Cancer Epidemiol., Biomarkers Prev. 2006; 15:1159–1169. [PubMed: 16775176]
69. Boyd NF, et al. Mammographic densities as a marker of human breastcancer risk and their use in chemoprevention. Curr. Oncol. Rep. 2001; 3:314–321. [PubMed: 11389815]
70. Boyd NF, Lockwood GA, Byng JW, Tritchler DL, Yaffe MJ. Mammographic densities and breast cancer risk. Cancer Epidemiol. Biomarkers Prev. 1998; 7:1133–1144. [PubMed: 9865433]
71. Parekh A, Weaver AM. Regulation of cancer invasiveness by the physical extracellular matrix environment. Cell Adhes. Migr. 2009; 3:288–292.
72. Wolf K, et al. Compensation mechanism in tumor cell migration: mesenchymal-amoeboid transition after blocking of pericellular proteolysis. J. Cell Biol. 2003; 160:267–277. [PubMed: 12527751]
73. Wyckoff JB, Pinner SE, Gschmeissner S, Condeelis JS, Sahai E. ROCK- and myosin-dependent matrix deformation enables protease-independent tumor-cell invasion *in vivo*. Curr. Biol. 2006; 16:1515–1523. [PubMed: 16890527]
74. Kessenbrock K, Plaks V, Werb Z. Matrix metalloproteinases: regulators of the tumor microenvironment. Cell. 2010; 141:52–67. [PubMed: 20371345]
75. Liotta LA, et al. Metastatic potential correlates with enzymatic degradation of basement membrane collagen. Nature. 1980; 284:67–68. [PubMed: 6243750]
76. Esserman LJ, Shieh Y, Park JW, Ozanne EM. A role for biomarkers in the screening and diagnosis of breast cancer in younger women. Expert Rev. Mol. Diagn. 2007; 7:533–544. [PubMed: 17892362]
77. Hwang ES, Esserman LJ. Management of ductal carcinoma *in situ*. Surg. Clin. North Am. 1999; 79:1007–1030. viii. [PubMed: 10572548]
78. Hadjantonakis A-K, Macmaster S, Nagy A. Embryonic stem cells and mice expressing different GFP variants for multiple non-invasive reporter usage within a single animal. BMC Biotechnol. 2002; 2:11. [PubMed: 12079497]
79. Inai T, et al. Inhibition of vascular endothelial growth factor (VEGF) signaling in cancer causes loss of endothelial fenestrations, regression of tumor vessels, and appearance of basement membrane ghosts. Am. J. Pathol. 2004; 165:35–52. [PubMed: 15215160]
80. Hutter JL, Bechhoefer J. Calibration of atomic-force microscope tips. Rev. Sci. Instrum. 1993; 64:1868.
81. Hertz H. On the contact of elastic solids. J. Reine Angew. Math. 1881; 92:156–71.

82. Costa KD. Single-cell elastography: probing for disease with the atomic force microscope. Dis. Markers. 2003; 19:139–154. [PubMed: 15096710]

Insight, innovation, integration

Tumors are stiffer than normal tissue, yet the individual tissue components that contribute to this biomechanical change remain undefined. We developed an *in situ* atomic force indentation microscopy approach to measure micron level stiffness in mammary tissues as they transformed. To identify the origins of the tissue stiffening we combined this method with live immunofluorescence imaging in a transgenic mouse model of mammary tumorigenesis. Our findings revealed that the epithelium, tumor-associated vasculature and the extracellular matrix each contribute to the mechanical landscape of the evolving tumor and that there was significant mechanical heterogeneity within the transformed tissue. The findings offer the first *in situ* quantitative analysis of the biomechanical forces that arise progressively within a tissue as it transforms.

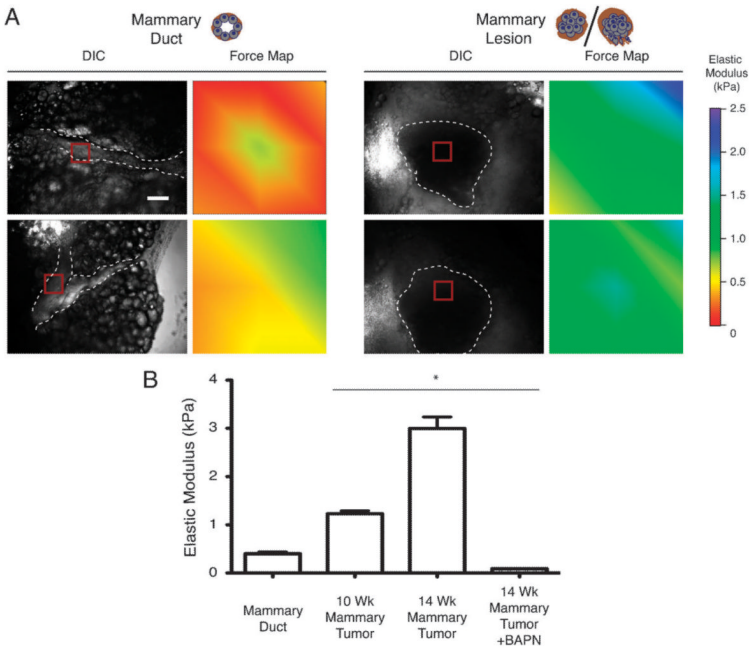

Fig. 1.

In situ biomechanical characterization reveals mammary tumors are stiffer than normal mammary ducts. (A) Representative DIC microscopy images showing mammary gland ducts (left column, dashed line) as compared to mammary lesions (right column, dashed line). AFM indentations were performed in 90 × 90 μm areas (red square) and the measurements obtained within this area are represented as a force heat map. Scale bar = 100 μm. (B) Bar graph demonstrating the average Young's elastic modulus calculated from force map measurements (see A). Error bars represent average ± S.E.M. *$P < 0.001$. Graphs represent compiled measurements taken from at least 5 mice. Each force map is made up of 36 indentations.

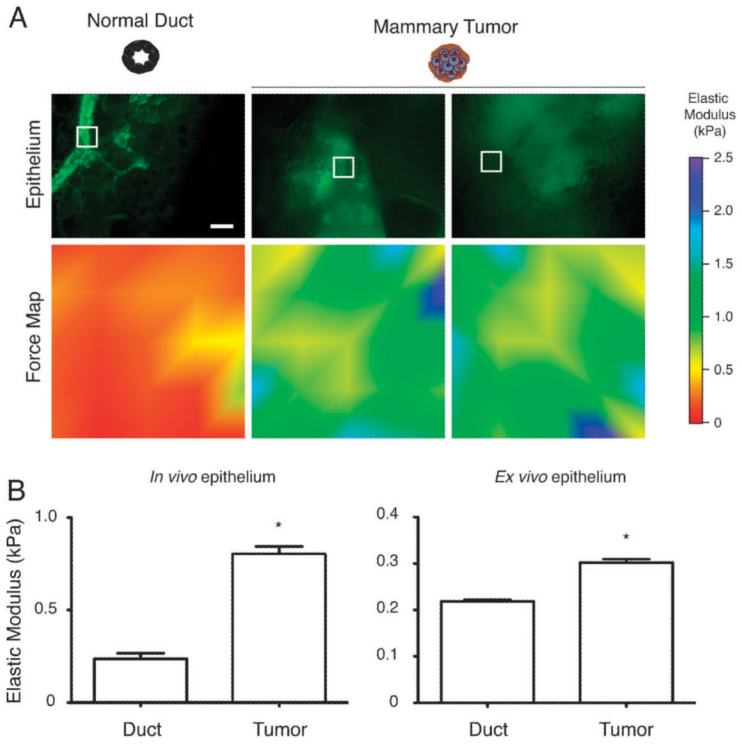

Fig. 2.

In situ biomechanical characterization reveals mechanical stiffening and heterogeneity of the tumor epithelium. (A) Representative fluorescence microscopy images showing mammary gland epithelium (green) tagged in the ACTB-ECFP transgenic mouse. AFM indentations were performed in 90 × 90 μm areas (white squares) and the measurements obtained within this area are represented as a force heat map. Scale bar = 100 μm. (B) Bar graph representing the Young's elastic modulus obtained by AFM indentation of *in situ* epithelium (left) or *ex vivo* cultured epithelium (right). Error bars represent average ± S.E.M. $*P <$ 0.05. Graphs represent compiled measurements taken from at least 8 mice. Each force map is made up of 36 indentations.

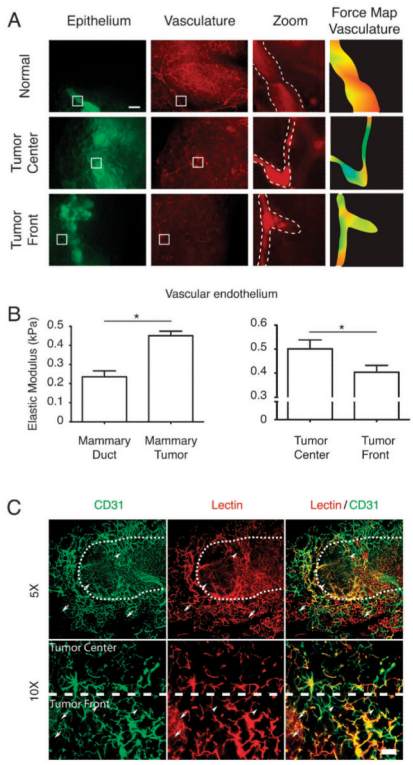

Fig. 3.

In situ biomechanical characterization reveals stiffening and mechanical heterogeneity of the tumor-associated vasculature. (A) Representative fluorescence microscopy images showing tissue vasculature labeled by Rh-lectin perfusion (red) and mammary gland epithelium (green) tagged in the ACTB-ECFP transgenic mouse. AFM indentations were performed in 90 × 90 μm areas (white square) and the measurements obtained within this area are represented as a force heat map. Only measurements corresponding to the vasculature (enclosed by dashed lines) were used during quantification. Scale bar = 100 μm. (B) Bar graph representing the Young's elastic modulus obtained from *in situ* vascular measurements obtained in (A). Error bars represent average ± S.E.M. $*P < 0.05$. (C) Representative fluorescent microscopy image showing CD31-stained vascluature (green) or patent vessel labeling by Rh-lectin (red). Adipose vessels with weak CD31 staining are indicated with arrows. CD31 stained, tumor-associated vessels that are not patent are indicated by arrowheads. Delineation of tumor center and tumor front is indicated by dashed line. Scale bar = 240 μm for upper panel and 120 μm for lower panel. Graphs represent compiled measurements taken from at least 12 mice. Each force map is made up of 100 indentations.

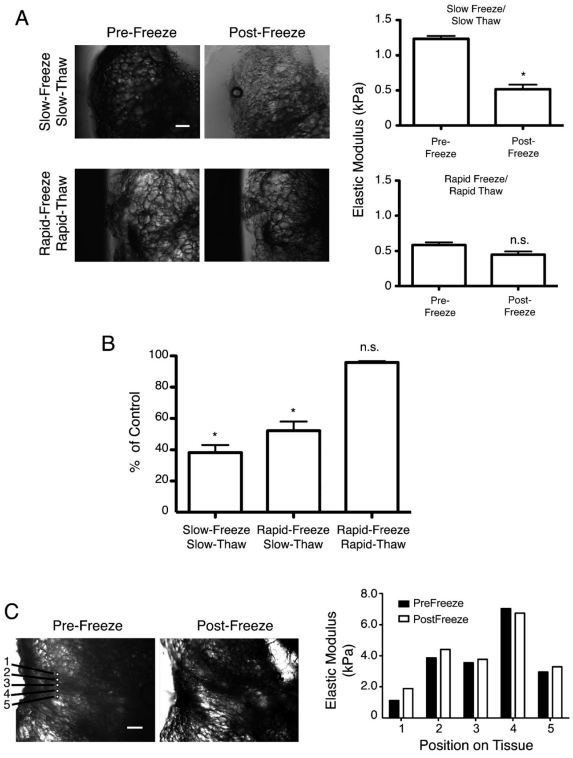

Fig. 4.

A novel vitrification approach to characterize ECM stiffness *in situ*. (A) DIC microscopy images showing rapid or slow frozen mammary gland tissues (left). Scale bar = 100 μm. Bar graph indicates the Young's elastic modulus calculated from frozen mammary gland tissues (right). Error bars represent average ± S.E.M. $*P < 0.05$. (B) Bar graph quantifying changes in tissue Young's elastic modulus when frozen by three different methods. Error bars represent average ± S.E.M. $*P < 0.05$. Graphs represent compiled measurements taken from at least 3 tissues. Each tissue was indented in 36 unique areas. (C) DIC microscopy images indicating five regions where AFM indentation was performed pre- and post-freezing (left). Scale bar = 100 μm. Bar graph quantifying changes in the Young's elastic modulus calculated from points (right). Error bars represent average ± S.E.M. $*P < 0.05$.

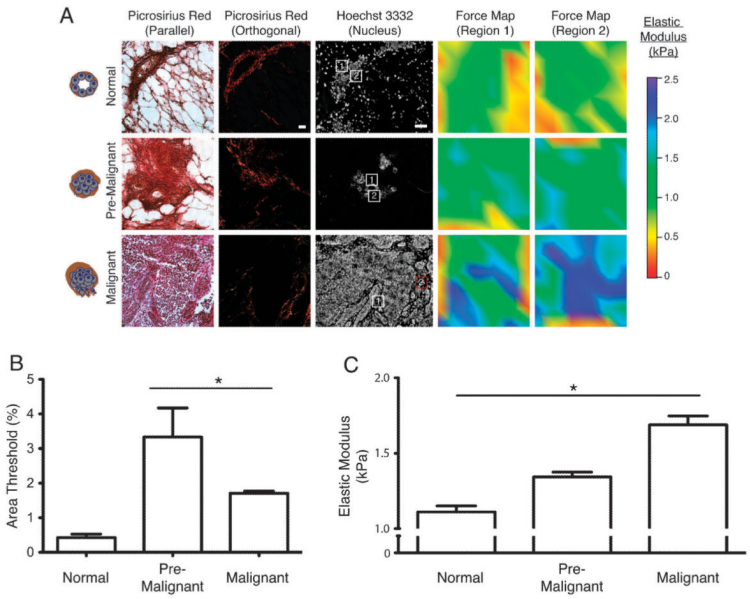

Fig. 5.

In situ biomechanical characterization reveals progressive ECM stiffening during tumor progression. (A) Picrosirius red microscopy viewed under parallel or orthogonal polarizing filters taken from mammary gland cryopreserved sections reveal the fibrillar collagen. Cell nuclei were identified by staining with Hoechst 3332. AFM indentations were performed in 90 × 90 μm areas (white squares) corresponding to ECM adjacent to the epithelium and the measurements obtained within this area are represented as a force heat map. Scale bar = 100 μm. (B) Bar graph representing quantification of fibrillar collagen deposition in tissues surrounding the mammary epithelium as % area threshold. Error bars represent average ± S.E.M. *$P < 0.05$. (C) Bar graph representing Young's elastic modulus of the fibrillar collagen adjacent to epithelium. Error bars represent average ± S.E.M. *$P < 0.05$. Graphs represent compiled measurements taken from at least 7 mice. Each force map is made up of 100 indentations.